Picosecond time-scale phase-related optical pulses: measurement of sodium optical coherence decay by observation of incoherent fluorescence

John T. Fourkas, William L. Wilson,* G. Wäckerle,† Amy E. Frost, and M. D. Fayer

Department of Chemistry, Stanford University, Stanford, California 94305

Received March 2, 1989; accepted June 6, 1989

A technique for producing phase-related picosecond optical pulses is described. A sequence of two phase-related pulses, well separated in time, is applied to the D_1 line in Na vapor. When the phase between the two pulses is scanned, oscillations in the incoherent fluorescence are observed. This demonstrates the well-defined phase relationship between the pulses. Measuring the amplitude of the oscillations as a function of pulse separation yields the Na optical coherence decay. A beat arising from the ground-state hyperfine splitting is observed, and the results agree well with calculation.

INTRODUCTION

The development of optical coherence techniques for probing the properties of systems of atoms and molecules has in many instances closely followed the path of development taken by nuclear magnetic resonance techniques. Optical pulses of well-defined duration, frequency, and amplitude have been employed. Some pulse sequences used in the optical regime, e.g., transient grating and coherent anti-Stokes spectroscopy experiments,[1,2] have no magnetic resonance analogs. In general, however, optical pulse sequences that parallel magnetic resonance have not been able to employ one important property of the pulses in most nuclear magnetic resonance sequences[3,4]: well-defined phase relationships. For instance, the photon echo, the stimulated echo, and other phase-independent techniques have been used to probe optical dephasing and population dynamics.[5–9] Additional information could be obtained with optical experiments analogous to various phase-related nuclear magnetic resonance sequences.

Phase-related optical pulse sequences in the microsecond and submicrosecond ranges have been employed by utilizing acousto-optic phase-shifting techniques to modulate cw lasers.[10–14] The fastest phase shifts in these experiments occur on a nanosecond time scale, however. Although nanosecond time-scale experiments are useful for probing gas-phase phenomena, many interesting condensed-phase phenomena occur on picosecond or femtosecond time scales. Thus it is desirable to be able to control the phase of pulses of these durations.

In solid-state applications, the simplest useful phase-related pulse sequence is a three-pulse fluorescence-detected photon echo.[14] This technique provides the same information as a normal (two-pulse) photon echo, but it has the advantage of being able to be applied to samples of poor optical quality because incoherent fluorescence is measured. This eliminates the need to detect a coherent pulse of light after it has passed through a sample of low optical quality. In such an experiment it is necessary only to be able to lock and scan the phase relationships among pulses; knowledge of the absolute phases is not required. The two-pulse experiments presented below could be precursors of a picosecond or femtosecond three-pulse fluorescence-detected photon echo.

The locking of the phase between temporally overlapping nanosecond and picosecond time scale pulses has been reported.[15,16] The technique used in the picosecond experiment is an interferometric one and will work only if the pulses overlap in time. For sequences such as the fluorescence-detected photon echo, however, it is necessary to lock the phase between pulses separated in time. Warren and co-workers have employed a technique based on a pulsed laser injection locked to a single-mode dye laser to generate phase-related pulses in the nanosecond and subnanosecond regimes.[17,18] Cw-laser-based techniques employing pulse-shaping methods and pulse compression have been used to produce pairs of phase-related pulses.[18,19] Here we report the successful phase locking of picosecond pulses with a method that, in principle, can be extended to subpicosecond pulses. The method can be applied to existing picosecond or femtosecond laser systems without incorporation of a cw laser.

To demonstrate the phase-locking method, a phase-related two-pulse sequence was applied to the D_1 Na transition and used to measure the Na optical coherence decay. A pulse from a tunable mode-locked dye laser is beam split to form the two pulses. The beams propagate along separate paths and are combined collinearly in the sample. On any single shot of the laser, there is a well-defined phase relationship between the pulses at the sample. The problem is to maintain that phase relationship over many shots of the laser. The phase fluctuations are relatively slow, i.e., less than 100 Hz (which is an order of magnitude slower than the laser repetition rate). Therefore it is possible to use a feedback system that compensates for time-dependent relative phase errors by driving a piezoelectric translator (PZT), which moves a corner cube along one of the beam paths, thus locking the phase relationship between the beams. Further

0740-3224/89/101905-06$02.00

along the beam path, a second PZT and another corner cube are used to scan the phase relationship between the pulses.

Na vapor has frequently been used as a proving ground for optical coherence techniques.[20] The two-pulse sequence is applied to the D_1 line in Na vapor to demonstrate the well-defined phase relationships between the pair of pulses. The first pulse puts the Na atoms into a coherent superposition of ground and excited states with a well-defined in-plane coherent component. After some evolution time (short relative to the free induction decay time), the second pulse arrives. Depending on the relative phase between the two pulses, the second pulse may leave the vector representing the in-plane coherent component unchanged or tip it upward or downward to some extent (corresponding, respectively, to increasing and decreasing the excited-state population). As the phase between the two pulses is slowly scanned, the probability of finding the system in the excited state after the arrival of the second pulse oscillates. Observation of the incoherent fluorescence intensity as a function of the phase shift reveals well-defined oscillations. This demonstrates the locking and scanning of the phase relationship between the pulses.

The depth of the fluorescence modulation with phase scan is determined by the magnitude of the in-plane coherent component at the time of the application of the second pulse. As the pulse-separation time is increased, the free induction decay reduces the amplitude of the in-plane coherent component, therefore reducing the amplitude of the fluorescence oscillation. The amplitude of the oscillations as a function of the pulse separation is proportional to the magnitude of the in-plane coherence. The use of incoherent emission to detect coherent effects was previously developed extensively in the context of optically detected magnetic resonance by Breiland *et al.*[21] Zewail and co-workers have performed fluorescence-detected photon echoes in a gas-phase sample on a nanosecond time scale.[14] Warren and Zewail have treated fluorescence-detected photon echoes theoretically.[22]

EXPERIMENTAL APPROACH

The experimental setup is shown in Fig. 1. Picosecond dye-laser pulses tuned to the Na D_1 line at 5896 Å are split into two equal pieces (the experimental beams) by a 50% beam splitter. One of these pulses traverses an optical delay line. On the delay line is a corner cube mounted upon a PZT, providing a means of changing the path length on an angstrom distance scale. This PZT is used to scan the phase between the split pulses by making slight path-length adjustments to the delayed pulse. The split beams are recombined collinearly with a 50% beam splitter. At this point the spot size ($1/e$ intensity diameter) of each beam is ~3 mm. The beams are passed through a 1-mm-diameter pinhole such that the variation of the intensity over the area of the pinhole is less than 10%. A lens is placed two focal lengths away from the pinhole to image the pinhole into a Na cell, which is also two focal lengths away from the lens. The pinhole is imaged as close as possible to the front window of the Na cell to avoid optical density effects. The cell is covered by heating wire and insulating material. The heating wires are used to keep the temperature at a constant value, in this case approximately 560 K. The solid Na is kept in a cooler sidearm of the cell, which is used to maintain the vapor pressure at approximately 10^{-6} Torr.[23] Holes in the insulating material at the front and rear windows of the cell allow the beam to enter and leave, and a 1-mm-wide vertical slit is left open on the side of the cell to allow the detection optics to view, at a right angle, the spot in the cell at which the pinhole is imaged. Fluorescence that emerges from the slit is detected by a thermoelectrically cooled phototube, a lock-in amplifier, and a computer (which is also used to control the phase-scanning PZT).

To stabilize the phase relationship between the pulse pairs, a small amount of each pulse is picked off by a beam splitter. The phase-scanning PZT is located farther along the beam path of the delayed beam than is the phase-locking pickoff. Thus only phase fluctuations caused by optics before the delay line can be corrected for; because of this, optics following the pickoffs are kept to a minimum. These picked off phase-locking beams are made time coincident and collinear by using another beam splitter. The intensity of this combined beam is then a sinusoidal function of the phase difference between the two pulses. The combined beam is detected by a photodiode. Another photodiode is used to detect an intensity reference beam, which is picked off elsewhere. The output of each photodiode is fed into its own sample-and-hold circuit, which is triggered at the laser repetition rate. The intensity reference signal is used to remove laser intensity fluctuations from the phase reference signal. The remaining fluctuations in the phase reference

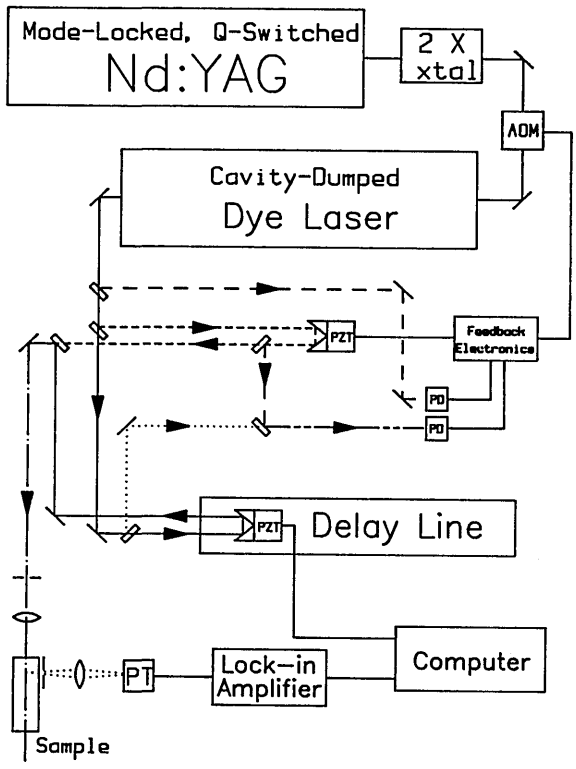

Fig. 1. Laser and experimental setup. A frequency-doubled acousto-optically Q-switched and mode-locked Nd:YAG laser pumps a cavity-dumped dye laser. The dye-laser pulses are split into two equal pieces, one of which is run down a delay line. The beams are recombined before the Na sample cell. Small portions of each beam are picked off, made time coincident, and recombined to make an interference pattern. This interference pattern, along with a picked-off intensity reference beam, allows the feedback electronics to stabilize the phase between the two pulses and the intensity fluctuations of the dye laser. AOM, acousto-optic modulator; PD's, photodiodes; PT, phototube.

signal are due to phase fluctuations between the phase-locking beams.

The timing (path length) between the phase-locking beams is adjusted such that the intensity of the combined beam is halfway between its maximum (constructive interference) and minimum (destructive interference) values. This maximizes the sensitivity of the phase reference signal to the phase fluctuations. This error signal is used to control a PZT-driven corner cube in the path of one of the experimental beams. If the error signal gain is adjusted properly, the PZT will compensate for phase fluctuations between the phase-locking beams, which are combined to form the phase reference beam. This locks the phase relationship between the experimental beams that give rise to the phase-locking beams. Thus the effects of phase fluctuations that occur at frequencies of the order of 100 Hz or slower can be removed. The major source of phase fluctuations is movement of optical components; since the mounts and other hardware are relatively massive, these fluctuations occur at low frequencies.

The computer scans the phase between the pulses by applying a ramp voltage to the phase-scanning PZT. Fluorescence data are simultaneously collected from the lock-in amplifier. The signal is not normalized for laser intensity fluctuations, although the computer may be used to average many scans to improve the signal-to-noise ratio.

Tunable pulses are generated by pumping a dye laser with the second harmonic of an acousto-optically Q-switched and mode-locked Nd:YAG laser. The dye laser is cavity dumped to produce single pulses of 40-psec duration and 0.3-Å bandwidth. A feedback circuit is used to reduce long-term dye-laser intensity fluctuations.

EXPERIMENTS AND RESULTS

Figure 2(a) displays fluorescence data taken as the phase between the two pulses exciting the Na sample is scanned. For these data the time delay between the excitation pulses is 107 psec, long enough to ensure that the two pulses do not overlap in time. Depending on the signal-to-noise ratio at a particular delay time, anywhere from 10 to 50 scans are averaged. The well-defined oscillations demonstrate the well-defined phase relationship between the two pulses.

To analyze the data quantitatively, initially consider the ground electronic state and the first excited state (the lowest energy component of the spin–orbit doublet) as a two-level system (hyperfine splitting neglected). The first pulse places each system in a coherent superposition of the ground and excited states, which is equivalent to rotating the Bloch vector toward the x–y plane and producing excited-state population. If the field is applied along the x axis in the rotating frame, the vector will be rotated toward the y axis in the y–z plane. Because the spectrum is inhomogeneously Doppler broadened (1.80 GHz FWHM), the ensemble begins to undergo free-induction decay (FID). The projection of the Bloch vector on the y axis shrinks. If the second pulse is brought in with a phase identical to that of the first pulse, the Bloch vector will be rotated further in the y–z plane toward the $+z$ direction. If, however, the phase of the second pulse is shifted 180°, the vector will be rotated back toward the $-z$ direction, because a phase shift in the lab frame appears as a change in the direction of the application of the field in the rotating frame. Phase shifting 180° is equivalent to applying the field along the $-x$ direction, and since the Bloch vector always rotates with the same sense around the field (or around the effective field if off resonance), the vector is rotated back down.

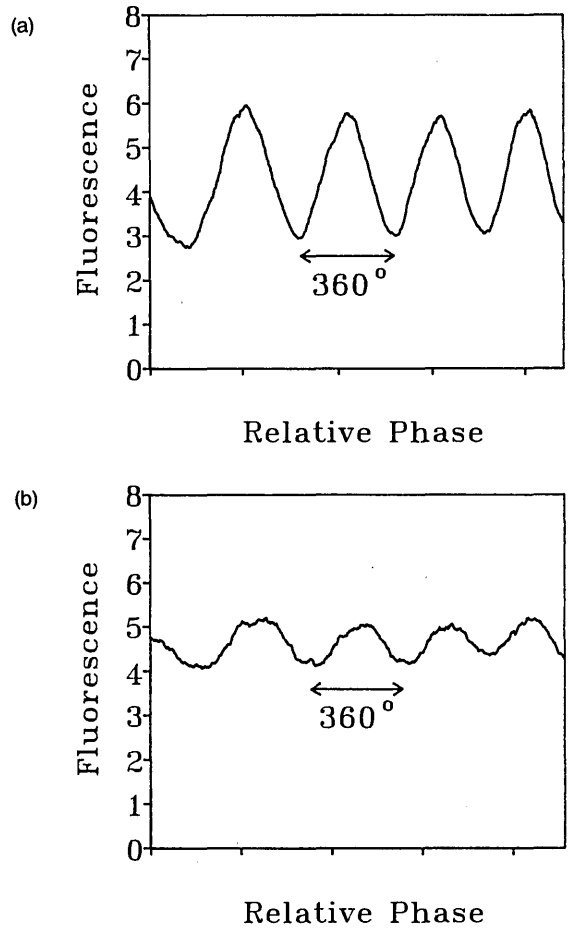

Fig. 2. (a) Fluorescence data from a two-pulse sequence as a function of relative phase. The delay between the two pulses was 107 psec. These data demonstrate the well-defined, scannable phase relationship between the pulses. The units of fluorescence are arbitrary. (b) Same as (a) but with a delay of 200 psec. The FID has reduced the intensity of the fluorescence oscillations.

To simplify the discussion, take the two pulses to be $\pi/2$, i.e., each moves the resonant Bloch vector through $\pi/2$ rad. After the first pulse the total Bloch vector points along y. The second $\pi/2$ pulse, having the same phase, rotates the vector to the $+z$ direction. For a given pulse delay this produces the maximum possible excited-state population, and subsequent fluorescence will be maximum in intensity. If the second pulse is phase shifted 180°, the vector is rotated to the $-z$ direction, and fluorescence is a minimum. Following the first pulse, the FID causes the length of the vector to shrink. Therefore all the population is not returned to the ground state by the second pulse, and there is still some fluorescence. As the relative phase is shifted through several cycles, the excited-state population (and hence the fluorescence) oscillates. This behavior is independent of the pulse intensities, which determine only the absolute amount of fluorescence.

Scans were taken from 16 to 66 mm along the delay line, corresponding to delays of 107 tp 440 psec between the pulses. Figure 2(b) shows data for a delay time of 200 psec.

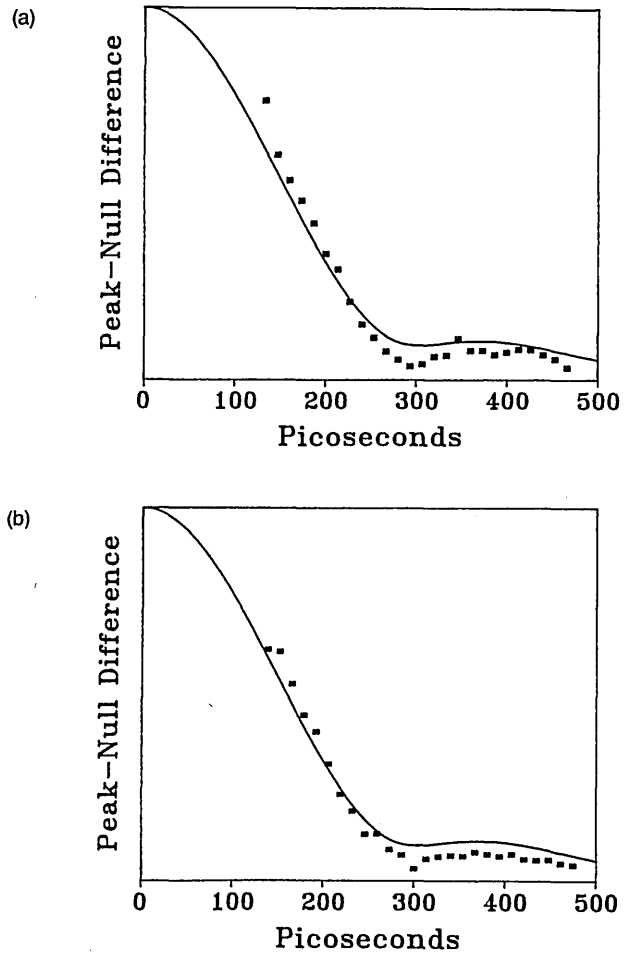

Fig. 3. (a) Average peak-null fluorescence difference as a function of delay between pulses. The pulse areas are 0.5π. The solid curves are a calculation based on the Na absorption spectrum and the laser bandwidth. The units of fluorescence are arbitrary. (b) Same as (a) but with pulse area of 1.2π. It can be seen that the data are qualitatively the same.

The extent of the oscillations is greatly reduced compared with that in Fig. 2(a).

The amplitude of the oscillations in the fluorescence depends on the extent of the FID. As the delay time between the two pulses increases, the in-plane component of the Bloch vector (polarization) shrinks, and the magnitude of the oscillations decreases. For large enough delays, the polarization disappears entirely, and the phase of the second pulse does not have an effect on the final state of the system. Therefore, by measuring the amplitude of the phase scan oscillations in the incoherent fluorescence as a function of pulse-delay time, the coherence decay can be measured.

For each scan, the height of each peak and each null is measured. The average null height is subtracted from the average peak height, and this difference is plotted as a function of pulse delay. Data of this type are plotted in Fig. 3. It can be seen that there is a beat in the coherence decay where the signal reaches a local minimum. The FID is the Fourier transform of the absorption spectrum and is equivalent to the coherence decay in certain cases. If the Na transition were actually a two-level system with Doppler broadening, the absorption spectrum would be a Gaussian, and the coherence decay would be the same as the FID. In reality, the ground and excited states are split by the hyperfine interaction. The excited-state splitting is 189 MHz,[24] which is smaller than the Doppler line width and is not observed. The ground-state hyperfine splitting, however, is 1.77 GHz. This splitting gives rise to a beat in the coherence decay. A single oscillation is observed because the FID has destroyed the polarization before another beat can occur. The solid curves through the data in Fig. 3 are from a calculation based on the known absorption spectrum of Na. The details of the calculation are given in the next section.

A FID contains both phase and amplitude information. The measurement made in this experiment contains only amplitude information. Therefore this technique cannot be used to reconstruct the FID. The relative phase between the two pulses is scanned through many cycles, and the fluorescence peak–null differences are recorded. However, when the phase-locking scheme is used the absolute phase difference between the pulses at each maximum and minimum in the fluorescence is unknown. The phase-locking scheme developed by Warren and co-workers[18,19] does allow one to know the absolute phase between pulses. As was discussed in the Introduction, to perform a fluorescence-detected photon echo it is unnecessary to know the phase relationship among the pulses. It is necessary only to lock the phase between pulses 1 and 2 and scan the phase between pulses 2 and 3. As in the experiments presented here, the information is contained in the amplitude of the oscillations in the incoherent fluorescence as a function of delay time between the pulses.

To test the power dependence of the experiment, data were taken at various pulse intensities. The data sets shown in Figs. 3(a) and 3(b) were taken with pulse energies of 1.5 and 7.8 nJ, respectively, which correspond to flip angles of 0.5π and 1.2π rad. Data were also taken at higher and lower powers. As can be seen from the figure, the data at these powers are basically the same, as is true for data taken at all powers.

THEORY AND CALCULATIONS

The experiments presented above will be described by using the density matrix formalism[25] following the notation of Warren and Zewail.[22] The density matrix is ρ, the radiation field frequency is ω_0, the electric field amplitude is E, the pulse duration is t, and the transition dipole moment is μ. The frequency offset $\Delta\omega$ and the Rabi frequency ω_1 are defined as

$$\Delta\omega = \omega - \omega_0 \tag{1}$$

and

$$\omega_1 = \mu E/\hbar. \tag{2}$$

Also, the flip angle θ and the flip axis ξ are defined by

$$\begin{aligned}\theta &= [(\Delta\omega)^2 + \omega_1^2]^{1/2}t \\ &\equiv \omega_{\text{eff}}t\end{aligned} \tag{3}$$

and

$$\begin{aligned}\xi &= \tan^{-1}(\omega_1/\Delta\omega) && \text{if } \Delta\omega > 0, \\ \xi &= \pi + \tan^{-1}(\omega_1/\Delta\omega) && \text{if } \Delta\omega < 0.\end{aligned} \tag{4}$$

At time $t = 0$, the atoms are in the ground state. This is represented by the density matrix

$$\rho(0) = \begin{bmatrix} 0 & 0 \\ 0 & 1 \end{bmatrix}. \tag{5}$$

The experiments described above were performed on the Na D_1 line. There is a 1.77-GHz ground-state hyperfine splitting and a 189-MHz excited-state hyperfine splitting. Therefore the Na D_1 transition is a transition not between two levels but rather among four. For high-power pulses, multiple transitions will be pumped up and down among the four levels. This general problem is not solvable. In the low-power (small flip angle) case, however, the problem simplifies and can be solved exactly. In the low-power limit, we assume that each isochromat is influenced only by the frequency component of the laser pulse that is at the resonance frequency of the isochromat. This is the linear regime of interaction of the radiation field with the atoms.

First we will calculate the response of a single isochromat to the pulse sequence. Because the laser pulse is a wave packet, all the different frequencies associated with the plane waves that make up the packet have well-defined phases relative to the center frequency of the packet. The center frequency is ω_0 and $\Delta\omega = \omega - \omega_0$. Because we are considering the low-power linear regime, each isochromat is driven as if it is interacting with an on-resonance field, i.e., the frequency component of the packet that is at the isochromat's transition frequency. The evolution of a two-level system under the influence of an on-resonance radiation field depends only on the area of the applied pulse, not on its shape; therefore the pulses can be taken to be square. In the frame of reference rotating at ω_0, however, each isochromat precesses during each pulse, and this much be taken into account. The flip angle of each isochromat depends on the amplitude of the field at $\Delta\omega$ and is denoted $\theta(\Delta\omega)$. The effective time during which the first pulse acts on the isochromat (length of the square pulse equivalent of the actual laser pulse) is t_1. With the initial condition given in Eq. (5), the density matrix after the first pulse is

$$\rho(t_1, \Delta\omega) = \begin{bmatrix} \sin^2[\theta(\Delta\omega)/2] & -i/2 \sin[\theta(\Delta\omega)]\exp(-i\Delta\omega t_1) \\ i/2 \sin[\theta(\Delta\omega)]\exp(i\Delta\omega t_1) & \cos^2[\theta(\Delta\omega)/2] \end{bmatrix}. \tag{6}$$

The system then evolves freely until time t_2. The density matrix is now

$$\rho(t_2, \Delta\omega) = \begin{bmatrix} \sin^2[\theta(\Delta\omega)/2] & -i/2 \sin[\theta(\Delta\omega)]\exp(-i\Delta\omega t_2) \\ i/2 \sin[\theta(\Delta\omega)]\exp(i\Delta\omega t_2) & \cos^2[\theta(\Delta\omega)/2] \end{bmatrix}. \tag{7}$$

The second pulse begins at t_2 and ends at t_3. Since we are interested in the fluorescence resulting from the two-pulse sequence, it is necessary to calculate the probability of the system's being in the excited state, i.e., $\rho_{11}(t_3, \Delta\omega)$. In the experiments, the flip angle is the same for the two pulses. The flip angle is a function of frequency, because the intensity of the laser pulse does vary somewhat over the Doppler-broadened width of the Na absorption. If we rename t_2 as τ (the time interval during which FID occurs), the probability [as a function of phase φ, the flip angle $\theta(\Delta\omega)$, and the time τ] of finding an isochromat of transition frequency $\Delta\omega$ in the excited state is

$$\rho_{11}(t_3, \Delta\omega) = \tfrac{1}{2} \sin^2[\theta(\Delta\omega)][1 + \cos(\varphi - \Delta\omega\tau)]. \tag{8}$$

Because the FID time is much shorter than the 16-nsec fluorescence lifetime,[26] emission before the end of the second pulse is not included in Eq. (8). Also, the experimental pressure is low enough that there are no collisions during the FID time.

Because the flip angle is small, $\sin[\theta(\Delta\omega)] \simeq \theta(\Delta\omega)$. This leads to the result that

$$\rho_{11}(t_3, \Delta\omega) = [\theta^2(\Delta\omega)/2][1 + \cos(\varphi - \Delta\omega\tau)]. \tag{9}$$

The flip angle at a given frequency is proportional to the electric field at that frequency. Since the frequency-dependent intensity, $I(\Delta\omega)$, is proportional to the square of the electric field at $\Delta\omega$, we find that

$$\rho_{11}(t_3, \Delta\omega) \propto I(\Delta\omega)[1 + \cos(\varphi - \Delta\omega\tau)]. \tag{10}$$

Relation (10) is for a single isochromat at frequency $\Delta\omega$. We want to calculate the fluorescence from an ensemble of atoms distributed in frequency across a spectral line and interacting with a laser pulse with a frequency spread. Therefore it is necessary to integrate relation (10) over frequency with ρ_{11} weighted at each frequency by the probability that there is an isochromat at the frequency (spectral line shape) and by the intensity of the laser pulse at the frequency (laser pulse line shape). The laser pulses used in the experiments and a Doppler-broadened spectral line are both Gaussians. The laser intensity distribution has a standard deviation σ_I, and the spectral line σ_L. The center of the intensity distribution is at $\Delta\omega = 0$, and the center of the spectral line is at ω_L. Following the second pulse, the observed fluorescence, $F(\tau, \varphi)$, as a function of τ and φ is

$$\begin{aligned} F(\tau, \varphi) = A &\exp[-\omega_L^2/2(\sigma_I^2 + \sigma_L^2)] \\ &\times \{1 + \exp[-\tau^2\sigma_I^2\sigma_L^2/2(\sigma_I^2 + \sigma_L^2)] \\ &\times \cos[\varphi - \omega_L\tau\sigma_I^2/(\sigma_I^2 + \sigma_L^2)]\}. \end{aligned} \tag{11}$$

The factor A contains phase- and time-independent constants such as sample concentration, illuminated volume, and total laser intensity.

Equation (11) is for a single Doppler-broadened line. As discussed above, the Na D_1 line is split by the hyperfine interaction. Therefore it is necessary to incorporate the spectral line shape. The 189-MHz excited-state hyperfine splitting corresponds to a beat time of the order of 2.5 nsec. This is much longer than the FID time and so cannot be observed. It is necessary to take into account the ground-state splitting of 1.77 GHz, however. Furthermore, each ground-state energy level has degenerate magnetic sublevels (of multiplicities three and five). This degeneracy factor weights the amplitude of the two spectral lines that arise from transitions from each of the ground states. Taking the center frequency of the laser to be between the two peaks, we find that

$$F(\tau, \varphi) = A(1 + \exp[-\tau^2\sigma_I{}^2\sigma_L{}^2/2(\sigma_I{}^2 + \sigma_L{}^2)] \times \{0.625 \cos[\varphi - \omega_L\tau\sigma_I{}^2/(\sigma_I{}^2 + \sigma_L{}^2)] + 0.375 \cos[\varphi - \omega_L\tau\sigma_I{}^2/(\sigma_I{}^2 + \sigma_L{}^2)]\}). \quad (12)$$

Equation (12) is used to calculate the curves through the data in Figs. 3 without recourse to adjustable parameters. The beat is at approximately 300 psec. τ in this equation is measured from the leading edge of the first pulse. This is when the FID begins.

It can be seen from Fig. 3 that the agreement between the calculation and the experiment is reasonably good. While the calculation is done for the low-power (linear) limit, the agreement with high-power experiments is the same as with low-power experiments. The calculation is possible only in the low-power limit, where the experiment can be treated as the interaction of the radiation field with two levels. The results of a high-power calculation are unknown. Such a calculation would have to include the nonlinear interaction of the radiation field with the four-level system and the temporal shape of the laser pulses. The experimental data, however, show that the low- and high-power determinations of ρ_{11} cannot differ to any significant extent.

ACKNOWLEGMENTS

We thank W. S. Warren for his helpful comments and insights. This research was supported by the U.S. Office of Naval Research, Physics Division (N00014-89-J-1119) and by the National Science Foundation, Division of Materials Research (DMR 87-18959). John T. Fourkas thanks the National Science Foundation for a graduate fellowship. William L. Wilson and Amy E. Frost thank AT&T Bell Laboratories for graduate fellowships. Gerhard Wäckerle thanks the Deutsche Forschungsgemeinschaft for partial support.

* Permanent address, AT&T Bell Laboratories, 600 Mountain Avenue, Murray Hill, New Jersey 07974.

† Permanent address, 2. Physikalisches Institut der Universität Stuttgart, Pfaffenwalding 57, 7 Stuttgart 80/Federal Republic of Germany.

REFERENCES

1. H. J. Eichler, *Laser-Induced Dynamic Gratings* (Springer-Verlag, Berlin, 1986).
2. D. D. Dlott, Annu. Rev. Phys. Chem. **37**, 157–187 (1986).
3. A. Abragam, *The Principles of Nuclear Magnetism* (Oxford U. Press, London, 1961).
4. M. Mehring, *Principles of High-Resolution NMR in Solids* (Springer-Verlag, Berlin, 1983).
5. N. A. Kurnit, I. D. Abella, and S. R. Hartmann, Phys. Rev. Lett. **13**, 567–568 (1964).
6. J. Hegarty, M. M. Broer, B. Golding, J. R. Simpson, and J. B. MacChesney, Phys. Rev. Lett. **51**, 2033–2035 (1983).
7. T. W. Mossberg, R. Kachru, S. R. Hartmann, and A. M. Flusberg, Phys. Rev. A **20**, 1976–1996 (1979).
8. M. Berg, C. A. Walsh, L. R. Narasimhan, K. A. Littau, and M. D. Fayer, J. Chem. Phys. **88**, 1564–1587 (1988).
9. L. R. Narasimhan, D. W. Pack, and M. D. Fayer, Chem. Phys. Lett. **152**, 287–293 (1988).
10. M. J. Burns, W. K. Liu, and A. H. Zewail, in *Spectroscopy and Excitation Dynamics of Condensed Molecular Systems*, V. M. Agranovich and R. M. Hochstrasser, eds. (North-Holland, Amsterdam, 1983).
11. E. T. Sleva, I. M. Xavier, and A. H. Zewail, J. Opt. Soc. Am. B **3**, 483–487 (1986).
12. J. E. Golub, Y. S. Bai, and T. W. Mossberg, Phys. Rev. A **37**, 119–124 (1988).
13. T. E. Orlowski, K. E. Jones, and A. H. Zewail, Chem. Phys. Lett. **54**, 197–202 (1978).
14. A. H. Zewail, T. E. Orlowski, K. E. Jones, and D. E. Godar, Chem. Phys. Lett. **48**, 256–261 (1977).
15. H. E. Grieneisen, J. Goldhar, N. A. Kurnit, A. Javan, and H. R. Schlossberg, Appl. Phys. Lett. **21**, 559–562 (1972).
16. M. Mukherjee, N. Mukherjee, J.-C. Diels, and G. Arzumanyan, in *Ultrafast Phenomena V*, G. R. Fleming and A. E. Siegman, eds. (Springer-Verlag, Berlin, 1986).
17. F. Spano, M. Haner, and W. S. Warren, Chem. Phys. Lett. **135**, 97–102 (1987).
18. W. S. Warren and M. Haner, in *Atomic and Molecular Processes with Short Intense Laser Pulses*, A. D. Bandrauk, ed. (Plenum, New York, 1988).
19. W. S. Warren and M. S. Silver, in *Advances in Magnetic Resonance* (Academic, London, 1988), Vol. 12.
20. E.g., L. J. Rothberg and N. Bloembergen, Phys. Rev. A **30**, 820–830 (1984); T. Mossberg, A. Flusberg, R. Kachru, and S. R. Hartmann, Phys. Rev. Lett. **39**, 1523–1526 (1977); A. Flusberg, T. Mossberg, R. Kachru, and S. R. Hartmann, Phys. Rev. Lett. **41**, 305–308 (1978); J. E. Rothenberg and D. Grischkowsky, Opt. Lett. **10**, 22–24 (1985); T. S. Rose, W. L. Wilson, G. Wäckerle, and M. D. Fayer, J. Chem. Phys. **86**, 5370–5391 (1987).
21. W. Breiland, C. Harris, and A. Pines, Phys. Rev. Lett. **30**, 158–161 (1973).
22. W. S. Warren and A. H. Zewail, J. Chem. Phys. **78**, 2279–2297 (1983).
23. A. N. Nesmeyanov, *Vapor Pressure of the Elements* (Academic, New York, 1963).
24. L. Allen and J. H. Eberly, *Optical Resonance in Two-Level Atoms* (Wiley, New York, 1975).
25. R. Feynman, F. L. Vernon, and R. W. Hellwarth, J. Appl. Phys. **28**, 49–52 (1957).
26. B. P. Kibble, G. Copley, and L. Krause, Phys. Rev. **153**, 9–12 (1967).